Mutation of an A-kinase-anchoring protein causes long-QT syndrome

Lei Chen*, Michelle L. Marquardt†, David J. Tester†, Kevin J. Sampson*, Michael J. Ackerman†‡, and Robert S. Kass*§

*Department of Pharmacology, College of Physicians and Surgeons of Columbia University, New York, NY 10032; and †Departments of Medicine, Pediatrics, and Molecular Pharmacology and Therapeutics, Divisions of Cardiovascular Diseases and Pediatric Cardiology, Mayo Clinic College of Medicine, Rochester, MN 55905

Communicated by Andrew R. Marks, Columbia University College of Physicians and Surgeons, New York, NY, November 5, 2007 (received for review August 28, 2007)

A-kinase anchoring proteins (AKAPs) recruit signaling molecules and present them to downstream targets to achieve efficient spatial and temporal control of their phosphorylation state. In the heart, sympathetic nervous system (SNS) regulation of cardiac action potential duration (APD), mediated by β-adrenergic receptor (βAR) activation, requires assembly of AKAP9 (Yotiao) with the I_{Ks} potassium channel α subunit (KCNQ1). KCNQ1 mutations that disrupt this complex cause type 1 long-QT syndrome (LQT1), one of the potentially lethal heritable arrhythmia syndromes. Here, we report identification of (*i*) regions on Yotiao critical to its binding to KCNQ1 and (*ii*) a single putative LQTS-causing mutation (S1570L) in *AKAP9* (Yotiao) localized to the KCNQ1 binding domain in 1/50 (2%) subjects with a clinically robust phenotype for LQTS but absent in 1,320 reference alleles. The inherited S1570L mutation reduces the interaction between KCNQ1 and Yotiao, reduces the cAMP-induced phosphorylation of the channel, eliminates the functional response of the I_{Ks} channel to cAMP, and prolongs the action potential in a computational model of the ventricular cardiocyte. These reconstituted cellular consequences of the inherited S1570L-Yotiao mutation are consistent with delayed repolarization of the ventricular action potential observed in the affected siblings. Thus, we have demonstrated a link between genetic perturbations in AKAP and human disease in general and *AKAP9* and LQTS in particular.

potassium channel | protein kinase A

A-kinase-anchoring proteins (AKAPs) are scaffolding proteins that determine the subcellular localization of protein kinase A and enzymes that regulate the PKA pathway, such as phosphatases or phosphodiesterases, and other kinases, such as PKC and PKD (1, 2). The molecular complexes of target proteins and regulatory enzymes coordinated by AKAPs ensure efficient spatial and temporal control of the phosphorylation state of targeted proteins, which in turn governs a plethora of cellular events ranging from neuronal excitability and plasticity to cardiac rhythm and contractility (1, 3). In the heart, AKAP-mediated macromolecular complexes coordinate the phosphorylation state of at least three critical ion channel proteins: the ryanodine receptor, or intracellular calcium-release channel (4), the L-type calcium channel (5, 6), and the slowly activating delayed rectifier I_{Ks} potassium channel (7). Inherited mutations in each of these target channel proteins are now known to be linked causally to at least two heritable arrhythmia syndromes: catecholamenergic polymorphic ventricular tachycardia (8) and long-QT syndrome (LQTS) (9). However, despite the critical role played by AKAPs in coordinating the regulation of these ion channel proteins, to date, no AKAP mutations have been associated with these or any other channelopathies. In fact, no human disease has been associated with genetic perturbations of AKAPs.

Here, we focused on a possible role of *AKAP9*-encoded Yotiao in the etiology of LQTS because we previously reported that Yotiao forms a macromolecular complex with the slowly activating cardiac potassium channel (I_{Ks}) (7), a critical repolarizing pathway in the human heart. Variants of LQTS have been shown to be caused by mutations in the I_{Ks} channel α (KCNQ1, LQT1) (10) or β (KCNE1, LQT5) (11) subunits. Furthermore, the physiologic response of the heart to sympathetic nerve stimulation (SNS) requires PKA-dependent phosphorylation of the I_{Ks} channel, mediated in turn by the binding of Yotiao to the KCNQ1 carboxyl terminal (C-T) domain (7, 12). Patients with LQT1-causing mutations are vulnerable to LQT-precipitated cardiac events during exertion when SNS activity is increased (13). Mutations in *KCNQ1* that disrupt the interaction with Yotiao render the channel unresponsive to cAMP-dependent regulation (7, 13, 14). Given the critical role of the adaptor protein Yotiao in the regulation of the I_{Ks} channel, we postulated that *AKAP9* may represent a LQTS-susceptibility gene. We also speculated that the large size of the Yotiao protein (>200 kDa) has hindered patient screens.

We now report the (*i*) identification of the binding motifs on Yotiao that coordinate its interaction with KCNQ1 and (*ii*) discovery of a missense Yotiao mutation(S1570L), using targeted mutational analysis of the translated exons in *AKAP9* that encode the KCNQ1/Yotiao-binding domains in a large cohort of patients with genotype-negative LQTS. The S1570L mutation (*i*) disrupts but does not eliminate the interaction between the two proteins, (*ii*) reduces cAMP-induced KCNQ1 phosphorylation, and (*iii*) eliminates the functional response of I_{Ks} channels to cAMP. These reconstituted cellular consequences of S1570L-Yotiao are consistent with the disease phenotype, delayed repolarization of the ventricular action potential. Thus, we have demonstrated that an inherited AKAP mutation may be linked to human disease.

Results

Amino- and Carboxyl-Terminal Regions of Yotiao Contribute to KCNQ1 Binding. Two Yotiao-binding regions for KCNQ1, one involving the Yotiao N terminus (residues 29–46) and the other within the Yotiao C terminus (residues 1,574–1,643) were identified initially by a combination of GST pulldown and immunoprecipitation (IP) experiments (data not shown). The roles of these two regions in coordinating Yotiao/KCNQ1 interactions were investigated by IP in a Chinese hamster ovary (CHO) cell line stably expressing KCNQ1 and transiently expressing full-length WT

Author contributions: L.C. and M.L.M. contributed equally to this work; L.C., M.L.M., M.J.A., and R.S.K. designed research; L.C., M.L.M., D.J.T., and K.J.S. performed research; L.C., M.L.M., D.J.T., K.J.S., M.J.A., and R.S.K. analyzed data; and L.C., M.L.M., K.J.S., M.J.A., and R.S.K. wrote the paper.

The authors declare no conflict of interest.

Freely available online through the PNAS open access option.

‡To whom correspondence may be addressed at: Windland Smith Rice Sudden Death Genomics Laboratory, Guggenheim 501, Mayo Clinic College of Medicine, 200 First Street SW, Rochester, MN 55905. E-mail: ackerman.michael@mayo.edu.

§To whom correspondence may be addressed at: Department of Pharmacology, College of Physicians and Surgeons of Columbia University, 630 West 168th Street, New York, NY 10032. E-mail: rsk20@columbia.edu.

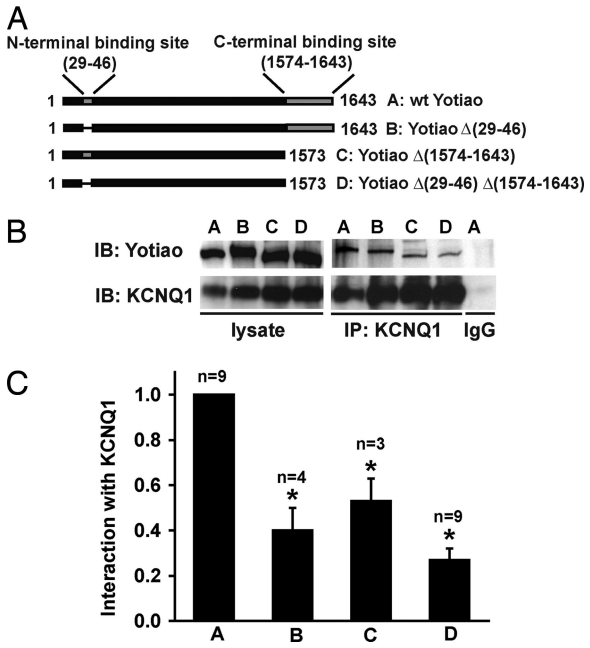

Fig. 1. Identification of KCNQ1-binding domains on Yotiao. (*A*) Two key binding sites for KCNQ1 on Yotiao, one on the N terminus (residues 29–46) and the other on the C terminus (residues 1,574–1,643), are shown in a schematic diagram. Four Yotiao constructs were used in the IP experiments to study the Yotiao/KCNQ1 interaction as shown in the diagram and described in *Results*. (*B*) A representative IP experiment demonstrates that both Yotiao N and C termini participate in the interaction with KCNQ1. An anti-KCNQ1 antibody was used to precipitate the KCNQ1/Yotiao complex. Control experiment was performed by using nonspecific goat IgG. Western blots (IB) of the lysates are shown (*Left*). Western blots of the immunocomplex are shown (*Right*). (*C*) The interactions between KCNQ1 and WT or mutant Yotiao were quantified by measuring Western blots of the immunocomplex, after correcting the IP input errors. Results were all normalized to WT Yotiao. *, $P < 0.001$; ANOVA and Bonferroni test.

Yotiao or its deletion variants (Fig. 1*A*). A KCNQ1 antibody was used to immunoprecipitate the KCNQ1/Yotiao complex. The two binding sites work cooperatively to coordinate Yotiao/KCNQ1 interactions. WT Yotiao (Fig. 1 *B* and *C*, construct A) IPs with KCNQ1. Deletion of the N-terminal binding site [Yotiao Δ (29–46), construct B in Fig. 1 *B* and *C*] reduces this interaction by ≈60% ($n = 4$), and deletion of the C-terminal binding site [Yotiao Δ (1,574–1,643), construct C in Fig. 1 *B* and *C*] reduces this interaction by ≈46% ($n = 3$). Deleting both binding sites further diminishes the KCNQ1/Yotiao interaction [Yotiao Δ (29–46)/Δ (1,574–1,643), construct D in Fig. 1 *B* and *C*, $n = 9$]. All Yotiao deletion mutants showed significant reduction in KCNQ1 binding compared with WT Yotiao ($P < 0.001$; ANOVA and Bonferroni test). Interestingly, the C-terminal binding site (1,574–1,643) contains a leucine zipper (LZ) motif that potentially matches a reciprocal binding site on KCNQ1, which is also a LZ.

Identification of a Yotiao Mutation in Patients with Familial LQTS. After a targeted mutational analysis of the exons (2, 9–11, and 16–19) of *AKAP9* (chromosome 7q21-q22) that encode these two KCNQ1-binding domains in Yotiao by using PCR, DHPLC, and direct DNA sequencing, a single putative LQTS-causing mutation (S1570L) in *AKAP9* (Yotiao) was identified in 1/50 (2%) Caucasian subjects with a clinically robust phenotype of LQTS (Table 1). The patients tested had been found not to carry mutations in any of the previously identified genes (LQT1–10) causally linked to LQTS including *KCNQ1* and *KCNE1*, and were thus noted as "genotype negative" (see *Methods*). Fig. 2 details the molecular characterization of the S1570L-AKAP9 missense mutation that was absent in 1,320 reference alleles (660 healthy white subjects), and localized to a functionally significant domain (KCNQ1-binding domain). Two of her sisters and their father have also been diagnosed with LQTS based on ECG. One sister (QTc = 480 ms) agreed to genetic testing and was positive for the S1570L-Yotiao mutation.

To be regarded as a putative LQTS-causing mutation, the genetic variant had to (*i*) be a nonsynonymous variant, (*ii*) be absent in at least 1,000 ethnic-matched reference alleles, and (*iii*) result in a functionally altered, proarrhythmic cellular phenotype. Consistent with the first prerequisite, synonymous single-nucleotide polymorphisms were excluded from consideration. To test for condition *ii*, control DNA obtained from the Human Genetic Cell Repository ($n = 200$ subjects) sponsored by the National Institute of General Medical Sciences and the Coriell Institute for Medical Research (Camden, NJ) and from a large cross-sectional, population-based study of predominantly Caucasians in Olmsted County, MN ($n = 460$ subjects) was analyzed. By using exact binomial confidence intervals for an allele frequency, absence of a variant of interest in at least 600 reference alleles indicates with a 95% confidence interval that the true allelic frequency is <0.5%, satisfying condition *ii*. We next tested for a S1570L-Yotiao proarrhythmic cellular phenotype.

Table 1. Demographics of unrelated genotype-negative patients with robust clinical phenotype for LQTS.

	Total cohort	S1570L index case
Number of unrelated patients	50	
Age at diagnosis, yr (range)	25.6 ± 15.9 (1–65)	13
Sex (male/female)	16/34	Female
Ethnicity (% white)	100	White
Average QTc, ms (range)	531 ± 60 (480–759)	485 ms
Average Schwartz and Moss score (ref. 22) (range)	3.75 ± 0.8 (3–5.5)	4
QTc ≥ 480 ms, %	100	
Syncope, %	46	Syncope
Cardiac arrest, %	14	
Positive family history, %	32	Positive family history
Positive family history of SCD, %	18	
Schwartz and Moss score ≥ 4, %	46	

Demographics for the 50 LQTS genotype-negative unrelated Caucasian individuals (34 females) with a clinically strong diagnosis of LQTS.

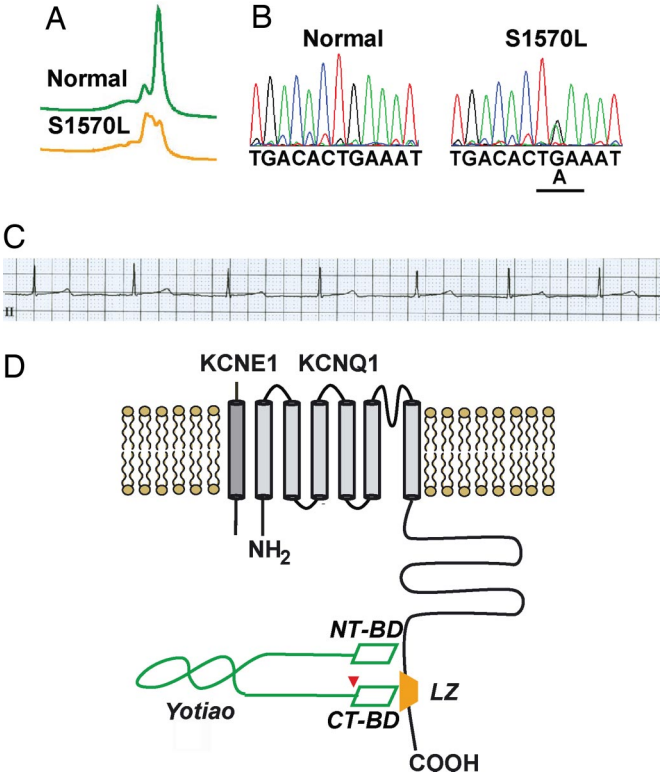

Fig. 2. A missense variant, S1570L, in *AKAP9*-encoded Yotiao in human LQTS. (*A*) DHPLC analysis of the DNAs from the patient positive for S1570L-Yotiao and normal controls. (*B*) Chromatograms of DNA sequences of the patient positive for S1570L-Yotiao and normal control. Underlined G-to-A change in nucleotide sequence causes the S1570L (serine, S, to leucine, L) missense mutation in Yotiao. (*C*) ECG of S1570L-Yotiao-positive patient with symptomatic LQTS (QTc, 485 ms). (*D*) A schematic diagram of the I_{Ks}/Yotiao complex. Shown in gray color in the plasma membrane are KCNQ1 and KCNE1, α- and β-subunits of I_{Ks}, respectively. A leucine zipper motif (LZ) is located at the C terminus of KCNQ1 and is the binding site for Yotiao. AKAP Yotiao is depicted in green. NT-BD and CT-BD indicate the two KCNQ1-binding sites on Yotiao N and C termini. The LQTS-associated mutation S1570L is located close to the CT-BD, indicated by an arrow.

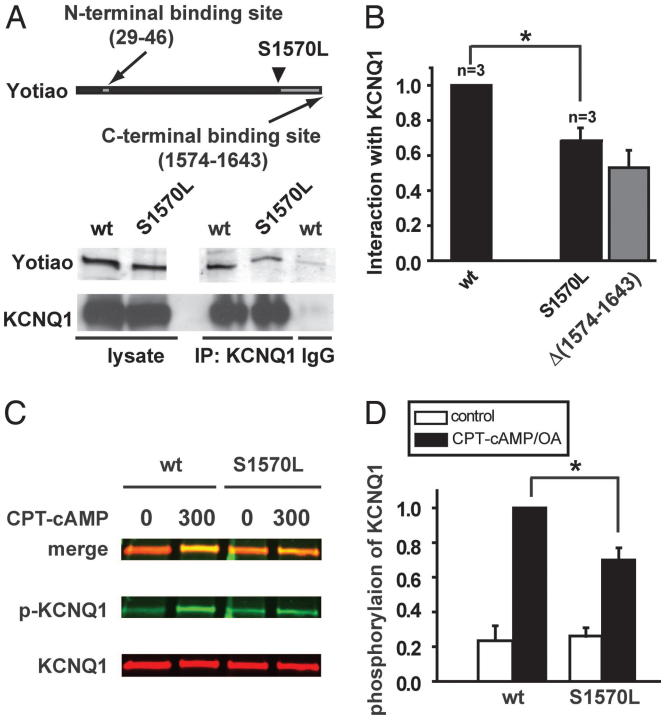

Fig. 3. S1570L Yotiao reduces the interaction with and the cAMP-dependent phosphorylation of KCNQ1. (*A*) An anti-KCNQ1 antibody was used to precipitate the KCNQ1/Yotiao complex from the lysates of the transfected CHO cells. A control experiment was performed by using nonspecific goat IgG. Western blots (IB) of the lysates are shown (*Left*). Western blots of the immunocomplex are shown (*Right*). (*B*) The interactions between KCNQ1 and either WT- or S1570L-Yotiao are quantified by measuring Western blots of the immunocomplex after correcting the IP input errors. Results are normalized to WT-Yotiao. The S1570L mutation significantly reduced the interaction between KCNQ1. *, $P < 0.05$ (paired *t* test). Yotiao and KCNQ1. *, $P < 0.05$ (paired *t* test). The gray bar represents the interaction between KCNQ1 and Yotiao Δ(1,574–1,643) reproduced from Fig. 1 and is for comparison purposes only. (*C*) Phosphorylation of KCNQ1 was assayed in the cells expressing KCNQ1 with either WT- or S1570L-Yotiao. Lysates were analyzed by dual Western blot by using an infrared imaging system. Green signals (*Middle*) detect phosphorylated KCNQ1 (*p*-KCNQ1) protein. Red signals (*Bottom*) detect total KCNQ1 protein. A merged view is presented (*Top*). (*D*) S27 phosphorylated KCNQ1 is quantified by measuring the relative band intensity on the phospho-KCNQ1 Western blots after correcting for total KCNQ1 loading. *, $P < 0.01$.

S1570L-Yotiao Modifies Yotiao/KCNQ1 Interactions and PKA Phosphorylation of KCNQ1. Using IP procedures in paired experiments, we compared WT- and S1570L-Yotiao interactions with KCNQ1. S1570L-Yotiao reduces the detected interaction with KCNQ1 (68 ± 7% compared with WT-Yotiao, $n = 3$, $P < 0.05$; paired *t* test, Fig. 3 *A* and *B*). This effect is similar to that of deletion of the C-terminal binding site shown in Fig. 1 [Yotiao Δ(1,574–1,643)] as illustrated in Fig. 3*B* by the light gray bar for comparative purposes only). We then tested whether S1570L-Yotiao might change cAMP-induced phosphorylation of KCNQ1. KCNQ1-expressing CHO cells were transfected with either WT- or S1570L-Yotiao and were treated with (+) membrane permeable cAMP (CPT-cAMP, 300 μM) plus okadaic acid (OA) or without (−)cAMP/OA (control), a procedure we have used to PKA phosphorylate KCNQ1 (15). We used an infrared fluorescence imaging system (see *Methods*) to detect and separate from a single gel signals from phosphorylated (green channel) and nonphosphorylated KCNQ1 channel protein (red channel), thus effectively reducing loading and detection errors (Fig. 3*C*). Cells transfected with S1570L-Yotiao showed a significant reduction in KCNQ1 phosphorylation in response to CPT-cAMP plus OA (Fig. 3 *C* and *D*).

S1570L-Yotiao Markedly Inhibits the Functional Response of I_{Ks} Channels to cAMP. I_{Ks} was measured before and after bath application of CPT-cAMP (50 μM) and OA (0.2 μM) in CHO cells cotransfected with KCNQ1, KCNE1, and either WT- or S1570L-Yotiao by using perforated-patch procedures. Fig. 4*A*, which compares the time course of the response of I_{Ks} channels to cAMP by measuring and plotting current amplitudes normalized to pre-cAMP challenge values vs. time, shows an I_{Ks} response when cells are transfected with WT- but not S1570L-Yotiao, a point reinforced by the averaged current traces illustrated in Fig. 4*B*. Fig. 4*C*, which plots mean I_{Ks} densities before and after application of CPT-cAMP/OA for cells transfected with either WT- or S1570L-Yotiao, reveals the following points. (*i*) Cells expressing S1570L-Yotiao had a lower I_{Ks} density (19.1 ± 3.2 pA/pF, $n = 8$) before CPT-cAMP/OA application compared with cells expressing WT-Yotiao (35.3 ± 6.1 pA/pF, $n = 14$, $P < 0.05$; Welch's *t* test). (*ii*) I_{Ks} densities in cells transfected with S1570L-Yotiao did not increase upon CPT-cAMP/OA application (19.1 ± 3.2 pA/pF before cAMP/OA, 17.1 ± 3.3 pA/pF after cAMP/OA, $n = 8$, n.s.; paired *t* test). (*iii*) I_{Ks} densities of cells transfected with WT-Yotiao increased upon CPT-cAMP/OA application (35.3 ± 6.1 pA/pF before cAMP/OA, 45.7 ± 9.0 pA/pF after cAMP/OA, $n = 14$, $P < 0.01$; paired *t* test). Thus,

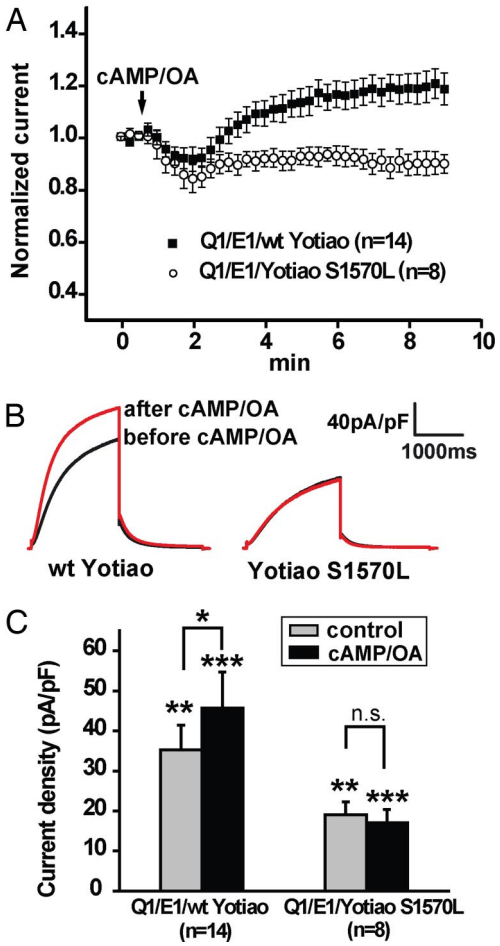

Fig. 4. S1570L-Yotiao markedly inhibits the functional response of I_{Ks} channels to cAMP. (*A*) Perforated-patch recordings were performed on CHO cells transiently expressing KCNQ1 and KCNE1 with either WT- (filled squares) or S1570L-Yotiao (open circles). Application of CPT-cAMP/OA was indicated by the arrow. Tail current amplitude was monitored and normalized to the current amplitude before application of CPT-cAMP/OA. Normalized tail current amplitude is plotted against time. (*B*) Average I_{Ks} current traces before (black) and after (red) application of CPT-cAMP/OA in cells transfected with WT-Yotiao (*Left*) or S1570L-Yotiao (*Right*) were shown. (*C*) Comparison of I_{Ks} tail current densities before (control, gray bar) and after (black bar) CPT-cAMP/OA treatment in cells transfected with either WT- or S1570L-Yotiao. Cells transfected with WT-Yotiao showed an increase in current density after CPT-cAMP/OA treatment (*, $P < 0.01$; control vs. cAMP/OA, paired *t* test). Cells transfected with S1570L-Yotiao did not respond to cAMP/OA (n.s. indicates no significant difference; control vs. cAMP/OA, paired *t* test). Basal (control) and cAMP/OA-treated I_{Ks} current densities in cells transfected with S1570L-Yotiao are significantly lower than that of the cells transfected with WT-Yotiao (**, $P < 0.05$; WT control vs. S1570L control, Welch's *t* test; ***, $P < 0.01$; WT cAMP/OA vs. S1570L cAMP/OA, Welch's *t* test).

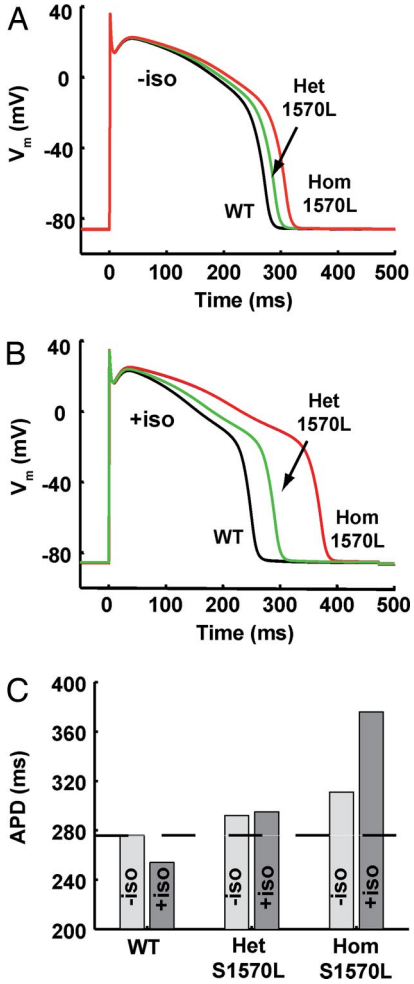

Fig. 5. S1570L-Yotiao is predicted to prolong action potential duration. (*A*) Simulations for steady-state action potentials stimulated at 1 Hz in WT (black line), heterozygous S1570L (green line), and homozygous S1570L (red line) cells show that the loss of functional translation of basal I_{Ks} complex phosphorylation leads to a APD prolongation (+35 ms for the homozygous cell). (*B*) In the presence of maximal isoproterenol stimulation, APD prolongation is severe in the mutant cells (+121 ms for the homozygous cell). (*C*) Significant APD prolongation is predicted in a gene dosage- and adrenergic stimulation-dependant manner.

I_{Ks} channels in cells transfected with S1570L-Yotiao are functionally unresponsive to cAMP.

Predicted Impact of the S1570L-Yotiao Mutation on the Electrical Activity in Ventricular Cardiocytes. To establish a causal relationship between the inherited mutation and its clinical phenotype, we performed computational analysis of cardiac action potentials based on the biochemical and biophysical data that we collected for S1570L-Yotiao and its impact on I_{Ks}. We used our previously developed model of I_{Ks} channel phosphorylation as a consequence of the β-adrenergic signaling cascade and its functional response to receptor stimulation (12). Here, we incorporated the signaling cascade end product into a model of human ventricular action potentials (16) to explore the predicted impact of the S1570L mutation. In the previous study, a small basal phosphorylation of the target proteins was predicted, including a phosphorylation of 13% of I_{Ks} channels, and so we used this value of basal I_{Ks} phosphorylation in the present computations. The S1570L mutation is modeled here as equivalent to the WT I_{Ks} complex in all aspects except its lack of response to channel phosphorylation. For a steady pacing rate of 1 Hz and no adrenergic stimulation, homozygous expression of the mutation would provide a 35-ms prolongation in action potential duration because of the removal of the effect of basal phosphorylation of the channel (Fig. 5*A*). For the same rate under maximal receptor stimulation, the discrepancy between WT and mutant cells grows to 121 ms. The computational data demonstrate a proarrhythmic cellular phenotype for S1570L-Yotiao and provide further evidence linking perturbations in *AKAP9* with LQTS.

Discussion

S1570L-Yotiao: An AKAP Mutation Linked to LQTS. Using targeted mutagenesis guided by a biochemical analysis of KCNQ1 and

Yotiao protein–protein interactions, we have identified a rare Yotiao missense mutation (S1570L) in an LQTS family that disrupts binding between KCNQ1 and Yotiao, reduces PKA phosphorylation of KCNQ1, eliminates the response of KCNQ1 to cAMP, and prolongs the action potential in computational models of the ventricular myocyte. Our findings thus support annotation of S1570L-Yotiao as a LQTS-susceptibility mutation rather than a polymorphism, and, as such, reports a disease-associated mutation of an AKAP.

The Interaction Between Yotiao and KCNQ1 and the Cellular Phenotype of S1570L-Yotiao. The interaction between Yotiao and KCNQ1 is required for the functional regulation of I_{Ks} channels in the face of an activated sympathetic nervous system, a process critical for maintaining normal heart rhythm. The molecular nature of the interaction is a three-way binding that involves the distal C terminus of KCNQ1 and both the N and C termini of Yotiao. Identification of the two KCNQ1-binding sites allowed us to quickly target the coding regions for these two important functional modules of the large Yotiao protein in patients with genotype LQT1–10-negative LQTS and laid the groundwork for the identification of the heritable missense mutation, S1570L, in Yotiao.

S1570L-Yotiao causes the following changes: (*i*) disruption, but not ablation, of the interaction between KCNQ1 and Yotiao, (*ii*) reduction of PKA-dependent phosphorylation of KCNQ1, and (*iii*) marked inhibition of the functional response of I_{Ks} current to cAMP stimulation. Disruption of the interaction between KCNQ1 and Yotiao by the mutation S1570L very likely explains the reduced PKA-dependent phosphorylation of I_{Ks} channel. The mutation-induced reduction in KCNQ1 phosphorylation thus reinforces the role of the AKAP Yotiao in facilitating local control of the phosphorylation state of the KCNQ1 protein. S1570L-Yotiao also markedly inhibits the functional response of the I_{Ks} channel to cAMP stimulation. This, in turn, as shown in the computer simulations, causes changes that are predicted to cause a prolonged cardiac repolarization period, a prediction that is manifested in the proband with a moderate degree of QT prolongation (485 ms) that exceeds the 99.5th percentile among women and is approximately the average QTc among patients with genetically proven LQTS.

S1570L-Yotiao partially reduces the cAMP-dependent phosphorylation of KCNQ1, but significantly blunts the functional response of the I_{Ks} channel to cAMP stimulation. What might be the underlying mechanism for the more pronounced effect of the mutation on channel function? One possibility is that the functional response of I_{Ks} requires phosphorylation of all (or some combination of multiple) KCNQ1 subunits within the tetrameric structure of the functioning channel, and this requirement may not be completely met when S1570L-Yotiao is substituted for WT-Yotiao, as reflected in the reduced phosphorylation we measure. However, we cannot detect putative subunit-specific phosphorylation changes within the tetramer to test directly for this possibility. In addition, synergistic effects with the active role of Yotiao downstream of channel phosphorylation may also contribute to the profound functional effect (17, 18). One potential downstream effect is that residue S1570 may be located in a Yotiao region of unknown active function that impacts the I_{Ks} channel or in a region that critically maintains the overall protein structure such that even a seemingly mild mutation at this position could result in marked alteration in transducing phosphorylation signal to channel function. Addressing this impact of the S1570L mutation will be the subject of future studies.

Insight into the Physiological and Pathophysiological Roles of AKAPs. Investigation into the mechanistic basis of inherited syndromes such as LQTS has provided strong evidence linking molecular systems to human physiology. The present study has extended these contributions by providing the first direct evidence that an inherited mutation of an *AKAP*-encoded protein can compromise human physiology (LQTS) and render the mutation carrier at risk for serious pathology (susceptibility to arrhythmia). We had speculated before that *AKAP9*-encoded Yotiao may be a candidate gene for LQTS, given its critical contribution to I_{Ks} regulation, but direct evidence has been lacking until this report. By using a combination of biochemical, molecular, and genetic analyses, we have been able to show that *AKAP9* is indeed a previously uncharacterized, albeit uncommon, LQTS-susceptibility gene. Our findings are not only relevant to further mechanistic understanding of LQTS, in particular, but to the appreciation of the physiological and pathophysiological roles of AKAPs in general. It is now clear that mutations of AKAPs can lead to life-threatening human disease.

Methods

LQTS-Negative Cohort. Between August 1997 and 2004, 541 consecutive, unrelated patients (358 females) were referred to the Mayo Clinic Windland Smith Rice Sudden Death Genomics Laboratory in Rochester, MN, for LQTS genetic testing (19). Clinical data including physical examination, personal history of syncope, seizures, or aborted cardiac arrest, family history, and 12-lead electrocardiogram (ECG) analysis were collected. Mutational analysis of the genes responsible for LQT1–10 was performed (19–21). Patients were characterized as either genotype-positive or -negative based on this primary analysis. This study focuses on the subset of 50 (34 females; average age at diagnosis 26 $\pm$ 16 years; average QTc 531 $\pm$ 60.4 ms; QTc range 480–759 ms) unrelated patients negative for LQT1–10 with a clinically robust phenotype of LQTS (QTc $\geq$480 ms or Schwartz score $\geq$3.0) (22).

***AKAP9* (Yotiao) Mutational Analysis.** After receiving written consent for this Mayo Foundation Institutional Review Board-approved protocol, genomic DNA was extracted from peripheral blood lymphocytes by using the Purgene DNA extraction kit (Gentra). A targeted mutational analysis of key *AKAP9* (chromosome 7q21-q22) exons (2, 9–11, and 16–19) encoding for the Yotiao domains that interact with KCNQ1 was performed on genomic DNA by using PCR, denaturing high performance liquid chromatography (DHPLC), and direct DNA sequencing.

Cell Culture and Transfection. CHO cells were cultured in Ham's F-12 culture media with 10% FBS in a 37°C incubator with 5% CO_2. Cells were transfected with Plus reagent and Lipofectamine (Invitrogen). For electrophysiology experiments, CD8 DNA was cotransfected with channel subunits and Yotiao cDNAs. Transfected cells were identified by using Dynabeads M-450 anti-CD8 beads (Dynal). We generated a CHO cell line that stably expresses KCNQ1 by using the Flp-In System (Invitrogen). The cell line was maintained in a media that contains Hygromycin B (500 μg/ml) and was used for biochemistry experiments (phosphorylation assay and immunoprecipitation).

Molecular Biology. Mutations were introduced into Yotiao by using the QuikChange site-directed mutagenesis kit (Stratagene) according to the manufacturer's protocol. All constructs were sequenced.

Phosphorylation Assay, Western Blot, Immunoprecipitation, and Antibodies. Phosphorylation of KCNQ1 in CHO cells was induced by incubating the cells at 37°C with 300 μM CPT-cAMP plus 0.2 μM okadaic acid (OA) for 10 min. Control experiments were performed without using CPT-cAMP and OA. Cells were then lysed in a 2$\times$ sample buffer (5% SDS, 75 mM urea, 300 mM sucrose, 50 mM TrisCl (pH 7.4) and 200 mM DTT) for 30 min in a cold room. The lysates were then incubated at 50°C for 5 min before being fractionized on SDS/PAGE gels. Dual Western blots were performed by using a rabbit anti-phospho-S27 (phosphorylated serine at position 27) KCNQ1 antibody (15) in combination with a commercial goat anti-KCNQ1antibody (Santa Cruz Biotechnology). An IRDye 800-conjugated donkey anti-rabbit IgG antibody (Rockland) and an Alexa Fluor 680-conjugated donkey anti-goat IgG antibody (Invitrogen) were used as secondary antibodies. Fluorescence signals of the phosphorylated and nonphosphorylated KCNQ1 were then detected simultaneously by using an Odyssey infrared imaging system (Li-Cor Bioscience) that offers wider linear range for detection and analysis. Western blot results were analyzed by using Odyssey software (Li-Cor).

For IP experiments, transfected cells were lysed in lysis buffer [150 mM NaCl, 10 mM Tris, 1 mM EDTA, 1% Triton X-100, pH 7.4, and Complete protease inhibitor mixture (Roche Applied Science)] at 4°C for 1 h. Lysates were then

centrifuged (15,000 × *g*) for 30 min (23, 24). Immunoprecipitation experiments were performed by using the supernatants with a modified radioimmune precipitation assay buffer (150 mM NaCl, 50 mM Tris, 1 mM EDTA, 0.25% Triton X-100, pH 7.5). A commercial KCNQ1 antibody (Santa Cruz Biotechnology) was used to IP and detect KCNQ1. Protein G beads were used to immobilize the immunocomplex. The immunoprecipitates were washed extensively by using RIPA buffer before being size-fractionized on SDS/PAGE. A Yotiao antibody was raised against a recombinant Yotiao fragment (residues 110–448) (Fusion Antibodies) to detect Yotiao in the immune complex. Western blot results were quantified by using ImageJ software (National Institutes of Health, Bethesda).

Electrophysiology. Perforated-patch experiments were performed 2 days after transfection to measure the functional I_{Ks} regulation in CHO cells. External solutions contain 132 mM NaCl, 4.8 mM KCl, 10 mM Hepes, 1.2 mM MgCl2, 2 mM CaCl2, 5 mM glucose, pH 7.4. The pipette solution contained 120 mM K-glutamate, 25 mM KCl, 10 mM Hepes, 1 mM MgCl2, 1 mM CaCl2 (pH7.2). Amphotericin B (Sigma) was included in the pipette (300 μg/ml) to perforate the cell. Cell perforation was judged by monitoring access resistance and usually took 10–15 min once a gigaohm seal was formed. Recordings started preferably when resistance dropped below 10 megaohms. Some recordings started when access resistance were between 10 and 15 megaohms. Holding potential was −70 mV. I_{Ks} was evoked and monitored by depolarizing the cell to +60 mV for 2 sec then repolarizing the cell to −40 mV for 2 sec. Current stabilization occurred within 5 min of patch perforation. Once the current stabilized, cells were perfused by 50 μM CPT-cAMP and 0.2 μM OA. I_{Ks} tail densities recorded at −40 mV were compared before and ≈9 min after drug application. Data were acquired and analyzed by using pCLAMP 8.0 software (Axon Instruments). Recordings were made at room temperature.

ACKNOWLEDGMENTS. We thank Dr. Howard Motoike for generating initial GST fusion proteins of Yotiao fragments. This work was supported by National Institutes of Health Grant R01HL 44365-12 (to R.S.K.), a Scientist Development Grant from the American Heart Association (to L.C.), the Mayo Clinic Windland Smith Rice Comprehensive Sudden Cardiac Death Program, the Dr. Scholl Foundation, and an Established Investigator Award from the American Heart Association (to M.J.A.).

1. McConnachie G, Langeberg LK, Scott JD (2006) *Trends Mol Med* 12:317–323.
2. Dodge-Kafka KL, Langeberg L, Scott JD (2006) *Circ Res* 98:993–1001.
3. Smith FD, Langeberg LK, Scott JD (2006) *Trends Biochem Sci* 31:316–323.
4. Marx SO, Reiken S, Hisamatsu Y, Jayaraman T, Burkhoff D, Rosemblit N, Marks AR (2000) *Cell* 101:365–376.
5. Hulme JT, Westenbroek RE, Scheuer T, Catterall WA (2006) *Proc Natl Acad Sci USA* 103:16574–16579.
6. Hulme JT, Lin TW, Westenbroek RE, Scheuer T, Catterall WA (2003) *Proc Natl Acad Sci USA* 100:13093–13098.
7. Marx SO, Kurokawa J, Reiken S, Motoike H, D'Armiento J, Marks AR, Kass RS (2002) *Science* 295:496–499.
8. Lehnart SE, Wehrens XH, Laitinen PJ, Reiken SR, Deng SX, Cheng Z, Landry DW, Kontula K, Swan H, Marks AR (2004) *Circulation* 109:3208–3214.
9. Moss AJ, Kass RS (2005) *J Clin Invest* 115:2018–2024.
10. Wang Q, Curran ME, Splawski I, Burn TC, Millholland JM, VanRaay TJ, Shen J, Timothy KW, Vincent GM, de Jager T, *et al.* (1996) *Nat Genet* 12: 17–23.
11. Abbott GW, Goldstein SA (2002) *FASEB J* 16:390–400.
12. Terrenoire C, Clancy CE, Cormier JW, Sampson KJ, Kass RS (2005) *Circ Res* 96:e25–34.
13. Schwartz PJ, Priori SG, Spazzolini C, Moss AJ, Vincent GM, Napolitano C, Denjoy I, Guicheney P, Breithardt G, Keating MT, *et al.* (2001) *Circulation* 103:89–95.
14. Piippo K, Swan H, Pasternack M, Chapman H, Paavonen K, Viitasalo M, Toivonen L, Kontula K (2001) *J Am Coll Cardiol* 37:562–568.
15. Kurokawa J, Chen L, Kass RS (2003) *Proc Natl Acad Sci USA* 100:2122–2127.
16. ten Tusscher KH, Noble D, Noble PJ, Panfilov AV (2004) *Am J Physiol Heart Circ Physiol* 286:H1573–1589.
17. Chen L, Kurokawa J, Kass RS (2005) *J Biol Chem* 280:31347–31352.
18. Kurokawa J, Motoike HK, Rao J, Kass RS (2004) *Proc Natl Acad Sci USA* 101:16374–16378.
19. Tester DJ, Will ML, Haglund CM, Ackerman MJ (2005) *Heart Rhythm* 2:507–517.
20. Sherman J, Tester DJ, Ackerman MJ (2005) *Heart Rhythm* 2:1218–1223.
21. Vatta M, Ackerman MJ, Ye B, Makielski JC, Ughanze EE, Taylor EW, Tester DJ, Balijepalli RC, Foell JD, Li Z, *et al.* (2006) *Circulation* 114:2104–2112.
22. Schwartz PJ, Moss AJ, Vincent GM, Crampton RS (1993) *Circulation* 88:782–784.
23. Carlisle Michel JJ, Dodge KL, Wong W, Mayer NC, Langeberg LK, Scott JD (2004) *Biochem J* 381:587–592.
24. Dodge KL, Khouangsathiene S, Kapiloff MS, Mouton R, Hill EV, Houslay MD, Langeberg LK, Scott JD (2001) *EMBO J* 20:1921–1930.